LET and Range Characteristics of Proton Recoil Ions in Gallium Nitride (GaN)

Jason M. Osheroff, *Member, IEEE*, Jean-Marie Lauenstein, *Member, IEEE*, and Raymond L. Ladbury, *Member, IEEE*

***Abstract*— A better understanding of the linear energy transfer and the range of proton recoil ions in gallium nitride is necessary to properly evaluate GaN device radiation tolerance.**

By analyzing the linear energy transfer (LET) and range of recoil heavy ions in GaN we can begin to reproduce the body of knowledge that exists for Si-based devices for this upcoming technology. Although the previous data on older technology has impressive depth and breadth we must be diligent and cautious in the application of these institutional intuitions when applied to emerging technologies such as GaN. As ever increasing materials science advances emerge, a sound methodology for evaluating new technologies must be established in order to apply what we know towards the effort of ensuring radiation tolerance.

***Index Terms*— gallium nitride (GaN), linear energy transfer (LET), proton testing, radiation effects, recoil ions, single event effects (SEE)**

I. Introduction

Gallium nitride (GaN) high electron mobility transistors (HEMTs) have received increasing attention among the space flight electronics community in recent years. While GaN offers superior electronic qualities in terms of higher electron mobility over Si and better thermal conductivity over gallium arsenide (GaAs), the radiation hardness of the latter technologies has been investigated for decades [1] and is generally well understood. One of the primary threats facing space flight electronics are single-event effects (SEE) caused by heavy-ion bombardment. Although galactic cosmic rays (GCR) are responsible for most of these events, these particles are typically more energetic than can be generated in a lab setting. As a compromise, lower-energy ions are used to generate similar effects. With these heavy-ion tests, in conjunction with engineering controls and statistical models, radiation hardness of electronics often can be reliably predicted. Over the last 15 years there has been extensive research and testing on GaN devices [2-7] for SEE and Displacement Damage Dose (DDD). Unfortunately, even these lower-energy heavy ions are produced at only a handful of facilities around the world. A far more commonly available energetic particle is the proton. Utilized heavily in the medical industry for therapy and diagnostic purposes, ~200 MeV protons are relatively accessible when compared to heavy ions [8]. Numerous studies have been conducted to understand the linear energy transfer (LET) of various ions in silicon that result from proton bombardment [9,10,11]. While these studies have yielded interesting results that answer many questions about proton-induced SEE from recoil ions in silicon-based technologies, they do not necessarily apply to the newer GaN technologies. Some studies [12] have begun to investigate the potential for SEE induced by proton irradiation in GaN.

Protons incident on a device deposit energy through direct ionization as well as elastic and inelastic scattering. The elastic and inelastic scatterings result in recoil ions that can be far more damaging than the initial proton. The energy loss to charge ionization from interaction of the ion with a material is generally quantified by the LET in units of MeV-cm^2/mg. This quantity depends on the target material, incident ion species, and energy. This means that we expect to see a difference in LET and particle range when performing heavy-ion tests on GaN devices as opposed to the more common Si devices. Not only are the effects of the ions different, but the energetic ions that are created via proton bombardment will differ from material to material. In silicon for instance, we expect ion species with atomic number Z=15 (phosphorus) and below as shown by Hiemstra [9]. The presence of ions with an atomic number one greater than that of silicon (Z=14) results from an inelastic collision between a proton and a silicon nucleus. Similarly for GaN we would expect to see recoil ions with an atomic number as high as 32 (germanium) resulting from an inelastic collision between a gallium (Z=31) nucleus and a proton. By exploring what ions are produced through these collisions, as well as elastic scattering of the Ga and N atoms, we can create a model for ionization caused by heavy ions in the material generated by incident protons.

II. Experimental Methods

A. SRIM

The transport code, *The Stopping and Range of Ions in Matter* (SRIM) [13], is used to calculate the LET for each ion that can be produced by proton irradiation of GaN. In theory we would expect the potential for inelastic scatterings to produce any element with a lower atomic number than the heaviest target nuclei, elastic scatterings with the elements that comprise the target, and finally recoil ions with atomic number

Manuscript submitted September 15, 2020. This work was supported in by the NASA Electronic Parts and Packaging Program (NEPP).

J.M. Osheroff, J.-M. Lauenstein, and R.L. Ladbury are with NASA/GSFC, Code 561.4, Greenbelt, MD 20771 (USA), (email: jason.m.osheroff@nasa.gov, jean.m.lauenstein@nasa.gov, and raymond.l.ladbury@ nasa.gov)

To be published in the Institute of Electrical and Electronics Engineers (IEEE) Transactions on Nuclear Science (TNS), April 2021.

one higher than the heaviest target nuclei produced from inelastic scattering. Technically heavier elements could be produced from subsequent inelastic collisions with these new, heavier nuclei but the probability is vanishingly low due to the scarce population of what in this case would be germanium. The data are plotted in Fig. 1 for recoil ion energies of up to 100 MeV. When compared with the analogous calculation in Si [9], it is apparent that the production of higher LET recoil ions is possible in GaN due to the heavier nuclei present in the target material.

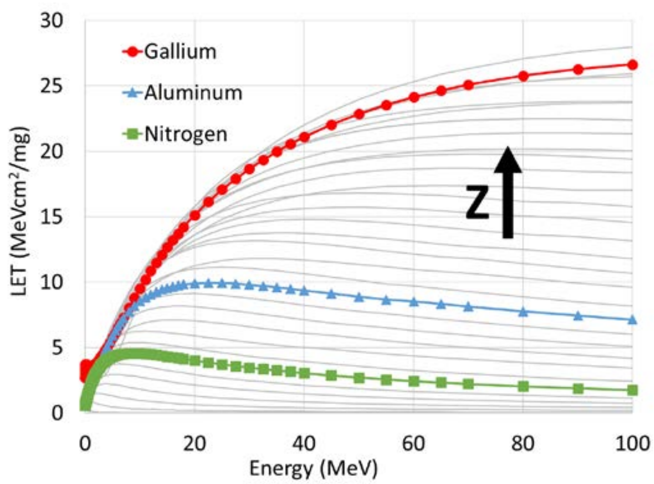

Fig. 1. LET in GaN of recoil ions resulting from proton bombardment as a function of recoil ion energy for ions Z=1-32. In general the LET increases with atomic number for a given energy, especially above 20 MeV. N, Al, and Ga are highlighted for reference.

Fig. 2 demonstrates that the ranges of the lighter ions can far exceed the dimensions of a typical GaN device (a few micrometers in thickness) while many of the heavier ions have ranges that are on the same order of magnitude of a typical device and more importantly reach higher LET in these ranges where they could potentially deposit significant energy in an SEE-sensitive volume.

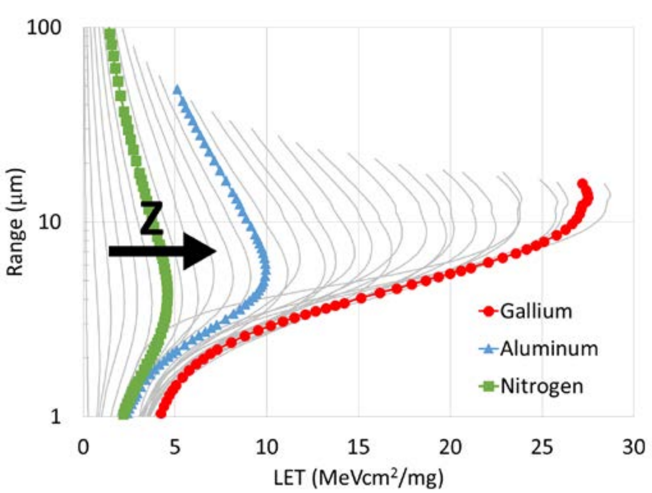

Fig. 2. Range in GaN of recoil ions resulting from proton bombardment as a function of recoil ion energy for ions Z=1-32. In general the traces from left to right have increasing atomic number. N, Al, and Ga are highlighted for reference.

B. Monte Carlo N-Particle Transport X (MCNPX) and (Los Alamos High Energy Transport (LAHET) codes

MCNPX [14,15] simulations were run for the scenario shown in Fig. 3 (left). The target stack is typical of a GaN HEMT consisting of a thin AlGaN layer on top of the bulk GaN. It is at the interface of these two materials where the Two-Dimensional Electron Gas (2DEG) is formed [16]. The proton source is a circular beam with a radius of 100 µm emitting protons at normal incidence to the top surface of the AlGaN layer and penetrating through the GaN layer below. Both layers are 1 cm by 1 cm wide to ensure that the entire beam is contained within the device. A range of proton energies was explored from 50 MeV up to 1 GeV to encompass environments that may be applicable to avionics, spaceflight hardware, and particle accelerator components. Fig. 4 shows a distribution of ions that were created in this scenario after $1x10^9$ simulated protons. The Monte Carlo N-Particle Transport X (MCNPX) code allows for transport of source particles through a user-defined geometry that takes into account electronic and nuclear interactions. This code was used in conjunction with the LAHET code [14,17] that was modified to include an output of the individual recoil ion species produced, including their energy and population information. When convolved with the SRIM results discussed above, the LET in GaN as well as the range of the proton recoil ions could be tabulated. The same procedure was repeated for a silicon target of the same dimensions to enable direct comparison.

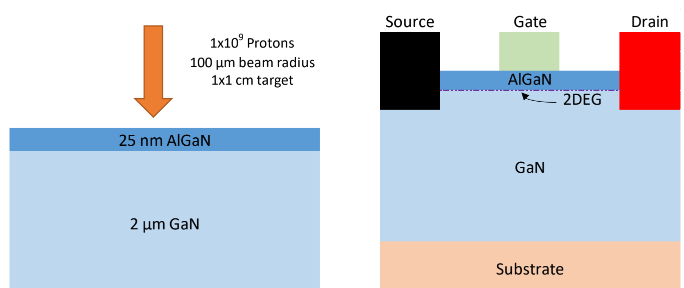

Fig. 3. (left) Scenario for MCNPX simulations, including the 200 MeV proton source and AlGaN/GaN target. (right) simple cross section of a typical GaN HEMT.

III. Results

A. Recoil Species

The mass and energy of the recoil ions will determine their LET and range. Fig. 4 shows a distribution of ions that were created in the GaN scenario shown in Fig. 3 after simulation of $1x10^9$ protons for the 50, 200, and 1000 MeV cases.

It is important to note that with previous studies in silicon [9,10,11] the highest-Z atoms present were phosphorus (Z=15) and Fig. 4 shows that, as anticipated, in GaN the highest-Z atoms present were germanium (Z=32). This finding indicates the possibility of higher LET recoil atoms arising during proton irradiation of GaN than during irradiation of Si, as suggested by Fig. 1. Not only are there higher-Z ions generated in this case but also the population of ions with atomic numbers ~24-32 clearly dominates the spectrum. Elastic recoils contribute significantly to the total recoil counts for Ga (Z=31) and N

(Z=7) but less so for Al (Z=13) due to the very thin AlGaN layer.

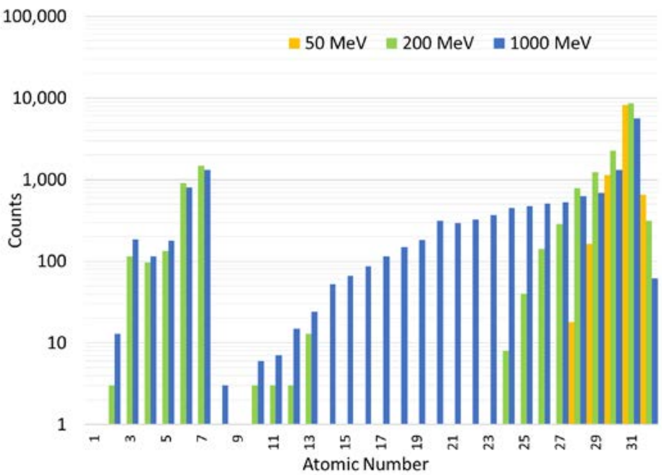

Fig. 4. Recoil production in AlGaN/GaN stack arranged by atomic number up to germanium (Z=32).

In an actual device there would be other contributions from metallization on the gate for instance. Metals such as gold used for this purpose could result in high-Z, high-LET ions but for this study only the AlGaN/GaN and bulk Si are examined to highlight the differences in the materials' behavior under irradiation.

Fig. 5 shows the distribution of ions that were created with a Si target of the same thickness (2.025 µm) and under the same conditions as the AlGaN/GaN stack for comparison.

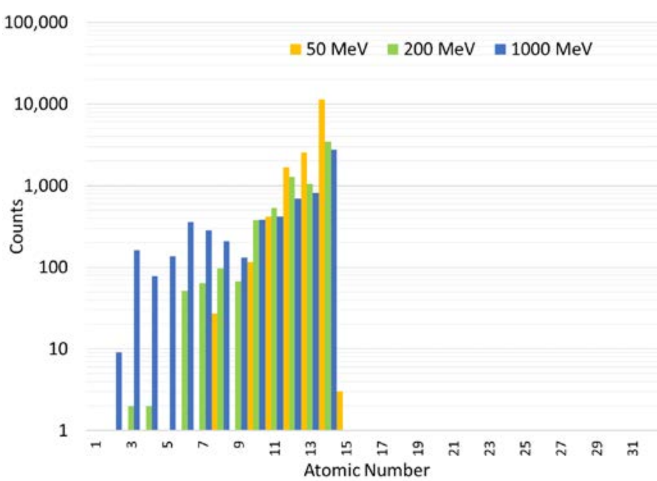

Fig. 5. Recoil ion production in Si stack from $1x10^9$ simulated protons.

As with the GaN simulation, the elastic Si recoils contribute significantly to the total counts for Z=14. However, it is worth noting that the inelastic collision with Si that results in phosphorus was very rare, occurring only a few times at low incident-proton energy while the production of germanium from gallium was in the hundreds of parts per billion (ppb). The germanium production also decreases with increasing incident proton energy as expected due to the lower interaction cross sections at higher energy but still occurs at a rate of 62 ppb.

Tabulating the total number of recoil ions over all species in Table I shows dramatic differences between the two target materials. The recoil production in Si vs. GaN, coupled with the difference in mass of the ions, illustrates how proton non-ionizing energy loss differs greatly in the two materials.

TABLE I
SECONDARY RECOIL ION PRODUCTION

Incident Proton Energy (MeV)	**50**	**100**	**200**	**500**	**1000**
Recoil ions in Si	16175	11964	6987	5897	6440
Recoil Ions in GaN	10178	20321	16385	25668	14883
Ratio (GaN/Si)	0.6	1.7	2.3	4.4	2.3

B. Linear Energy Transfer (LET)

While the heavy-ion population arranged by atomic number provides valuable insight into the particles that may cause potential SEE during proton irradiation, it does not tell the whole story. Although the heavier ions do have potentially higher LETs, these values are energy dependent as previously mentioned in section II. The LAHET code provides the ability to record the production of recoil ions from both elastic and inelastic collisions. For each recoil, the ion's energy information can be recorded in user-defined bins allowing for post-processing of the simulation data. The highest energy ions generated in GaN from 200 MeV protons were below 60 MeV, however, 1000 MeV protons resulted in elastic recoils of Ga as high as 83 MeV. By first converting the energy data provided by the LAHET code, then using the SRIM results to find the LET of each recoil ion, a table of ions within certain LET bins can be constructed.

Figs. 6 and 7 show a combination of all ion species categorized by the LET corresponding to the energies of each species present in Si and GaN respectively according to the MCNPX and LAHET code**s**. Surprisingly, the maximum LET of the recoils resulting from 200 MeV protons on the GaN target is only 13 MeV-cm^2/mg, similar to that found for silicon.

In addition, at the higher LETs, there is almost an order-of-magnitude more recoils in Si than in GaN. This story changes dramatically as the proton source energy is increased above 200 MeV.

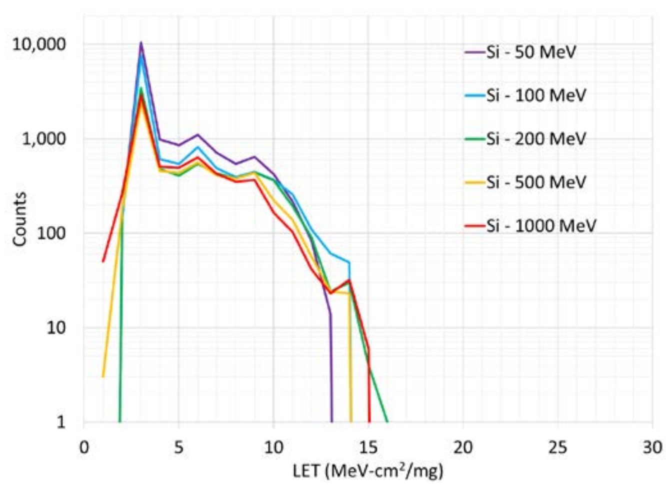

Fig. 6. Secondary production in Si target. Bin labels shown reflect the upper bound on LET of each bin.

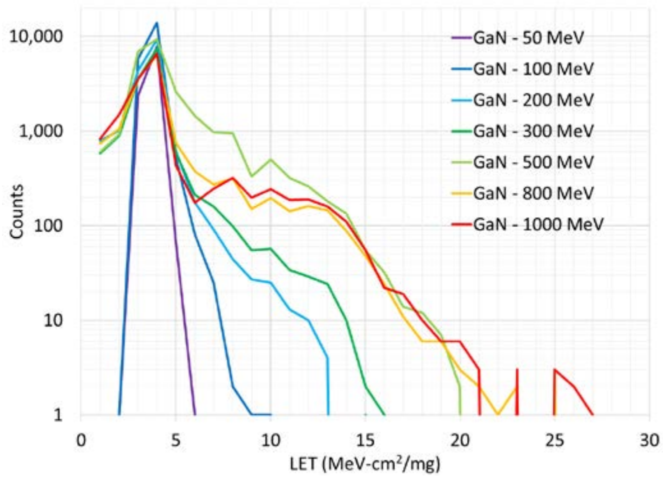

Fig. 7. Secondary production in AlGaN/GaN stack. Bin labels shown reflect the upper bound on LET of each bin.

Investigating individual recoils shows that the low LET peaks for both Si and GaN originate from the high angle (glancing) elastic recoils of Si and Ga respectively while the high LET contributions to the GaN LET spectrum come from low angle (head-on), high energy transfer elastic collisions. To understand why this phenomenon dictates the different proton energy dependences between the two target materials we analyze the head-on maximum energy transfer elastic collision.

Looking at the conservation of energy and momentum laws for head on elastic collisions:

$$E_{i-proton} = E_{f-proton} + E_{f-target} \quad (1)$$

$$p_{i-proton} = p_{f-proton} + p_{f-target} \quad (2)$$

Where the kinetic energy (E) and momentum (p) are given for the incident *proton* and *target* material before and after collision denoted by the subscripts '*i*' and '*f*' respectively. We can substitute the relationship between energy and momentum where 'm' is the mass of the proton or target:

$$E = \frac{p^2}{2m} \quad (3)$$

And solve for the final energy of the target nucleus as a function of the incident proton energy and masses of the proton (m_{proton}) and target (m_{target}).

$$E_{f-target} = E_{i-proton} * \frac{4m_{proton}}{m_{target}\left(1-\frac{m_{proton}}{m_{target}}\right)^2} \quad (4)$$

From this calculation we see that the maximum recoil ion energy for a given incident proton energy is simply a function of the target mass with respect to the proton mass. Plugging in values for Si and Ga targets reveals:

$$E_{Si\_Recoil} \approx 0.153 * E_{i-proton} \quad (5)$$

$$E_{Ga\_Recoil} \approx 0.059 * E_{i-proton} \quad (6)$$

This gives an upper bound for the recoil energies for Si and Ga respectively. While at first glance one notes that the Si atoms gain more energy from the protons (about 15% compared to 6% for Ga), we know that the LET is dependent on the mass of the recoil ion. Using these relationships and the LET as a function of energy information obtained from SRIM we plot the recoil ion as a function of incident proton energy for each species in Fig. 8.

This shows that while the Si recoils are capped at an LET of about 14 MeV-cm^2/mg resulting from proton bombardment below 200 MeV the possible Ga recoils continue to increase in LET beyond 1000 MeV reaching values of 27.5 MeV-cm^2/mg resulting from ~2800 MeV incident protons. While most accessible proton sources for radiation testing produce 200 MeV particles, only the most powerful research grade accelerators in the world are capable of energies over 1 GeV. This poses challenges for simulating the space radiation environment in a laboratory setting as GCR can have energies of several GeV per nucleon [18].

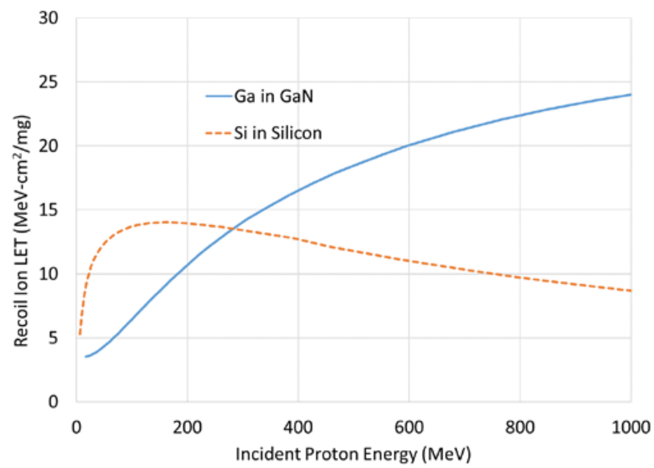

Fig. 8. Upper bound for elastic recoil ion LET in Si and GaN as a function of incident proton energy.

It is important to note that the GaN target material also includes nitrogen atoms that generate recoils as well. Due to the low atomic number of nitrogen the elastic recoils do not contribute to the high LET ions and are only capable of delivering about 5 MeV-cm^2/mg. Likewise, there is little emphasis on the contribution of Al recoils in this work. One would expect Al recoils to behave similarly to Si due to their similar atomic number. This could result in an increase in ions with LET values of 5-15 MeV-cm^2/mg from low-energy proton beams but would not contribute meaningfully to the high end of the spectrum where recoil ions in GaN exceed the LET of those in Si. While this study uses a single thin AlGaN layer with equal amounts of Al and Ga, there has been work [19,20,21] investigating alternative mole fractions and if the population of Al in such a device were to become significant enough we would expect to see some changes on the lower end of the spectrum as described.

The difference between Figs. 6 and 7 illustrates the key finding of this work: While the LET spectrum for Si exhibits very little dependence on the incident proton energy, the spectrum for GaN is greatly impacted. As the proton energy increases, there is also an increase in the production of higher LET recoil ions in GaN. For "mid-range" LET (between 10-20 MeV-cm^2/mg) the effect eventually saturates around 500 MeV. However, the highest LET recoils produced in a group continue to increase reaching as high as 27.5 MeV-cm^2/mg as compared to the highest recoil produced in all of the Si trials at 16 MeV-cm^2/mg.

This could imply that test standards for silicon that dictate when proton tests need to be conducted in order to incorporate event rates from on-orbit protons will need to be adjusted:

1) to a different LET threshold, possibly 27.5 MeV-cm^2/mg rather than 15 or 20 MeV-cm^2/mg currently used and,
2) that the full susceptibility may not be possible to experimentally identify due to available proton facility energy limitations.

C. Range

In addition to the LET data displayed in Figs. 6 and 7, the range information for each ion can be compiled across recoil ion species to show the distribution of ion ranges produced as shown in Fig. 9. The results for GaN and for Si from the 200-MeV protons are similar. The majority of the recoil ion ranges are on the order of a typical GaN HEMT device size or shorter, providing good confidence that the majority of energy will be deposited within the HEMT near the location of the recoil production. In contrast, a silicon SEE-sensitive volume can be much larger than the recoil range depending on the device and effect [11, 22]. We can further dissect these data to find that most of the ions with high LET (>10 MeVcm^2/mg) have a range in GaN of between 2-4 μm. In contrast, for Si, this range is between 4-8 μm.

While a 2 μm thick GaN layer was used in this simulation, incident angle and impact location can result in longer path lengths in the device. In addition, as GaN devices continue to be developed, different thicknesses, substrates, Al mole fractions, etc., are to be expected. Many of the impacts of these variations as they relate to ion range are discussed by Mizuto [23]. For this reason Fig. 9 highlights the ranges of ions centered on this 2 μm baseline.

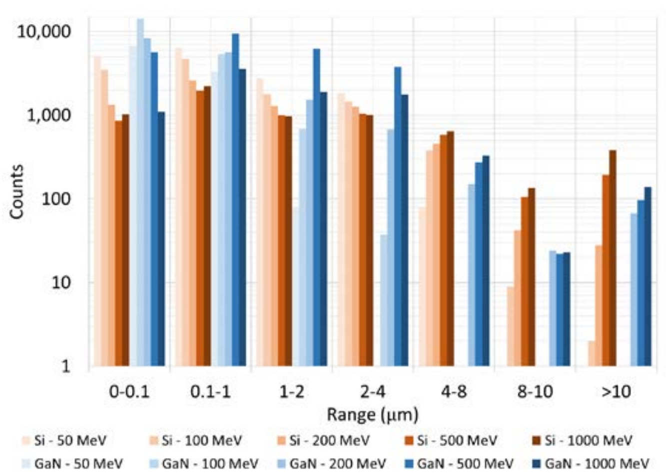

Fig.9. Recoil ion ranges in GaN resulting from bombardment with 1x10^9 protons.

IV. Conclusions

Comparison of these simulations with previous work in Si [9,10,11] shows key differences in the range and LET of proton recoil ions in GaN as a function of proton energy. It has been demonstrated that the species and population of these ions in the two materials varies significantly, precluding the blanket application of models for Si-based technologies to GaN. In addition, radiation test methods and requirements developed for Si microelectronics may not be appropriate for GaN devices due to the recoil production differences under proton irradiation. In this work, an independent model for energetic proton irradiation of GaN devices is established and resulting energy deposition predicted. This information provides a clearer understanding of the secondary processes occurring during proton irradiation of GaN devices that may lead to SEE.

Many proton studies are focused on the energy deposited by the proton [24], which is very valuable, but knowledge about the potential high-LET secondary ions produced by the protons may also be of consequence at higher energies. While these studies are often targeting low-energy protons (1-100 MeV) to emulate on-orbit flux spectrums from trapped and solar protons this work suggests the potential utility of high-energy proton tests to probe other damage mechanisms in GaN devices. Due to the resilience of bulk GaN to Total Ionizing Dose (TID) [25] it is feasible that high-energy proton irradiation could be applied at high enough fluence to generate a sufficient quantity of high LET (>20 MeV-cm^2/mg) ions to gather SEE data similar to what would be seen at a heavy-ion facility. Several studies have been conducted and analyzed [26-29] examining the effects of high fluence (1x10^{13} – 1x10^{16} protons/cm^2) and TID on electrical parameter shift. This data can help determine tolerable fluence levels that, as shown in this work, could result in appreciable high LET recoil ions.

By examining the LET and range of recoil ions as a function of incident proton energy we can also draw some conclusions about applications to different industries relying on radiation hardened electronics. Space applications are generally concerned with protons below 300 MeV as evidenced by the models used to predict radiation threats to spacecraft [30]. In this lower energy regime we can see from the simulations that recoil ions in GaN do not yet exceed LET values we are used to seeing in Si. This suggests that for space applications where protons in excess of 300 MeV are rare, institutional knowledge of proton testing for Si may be applied to GaN technologies and yield conservative estimates as far as secondary recoil ions are concerned. However, in applications that involve higher-energy protons GaN begins to experience higher-LET recoils with respect to Si. By 500 MeV, significantly higher-LET ions are generated and this trend continues well beyond 1 GeV.

While high-energy protons (>500 MeV) may not warrant consideration in most space environments due to their scarcity, there are particle accelerator and collider environments that could have electronics affected by such interactions. For instance, GaN-based accelerator components exposed to a high energy proton beams could experience recoil ions with nearly double the LET of their Si counterparts. As new technologies emerge it is crucial to constantly reevaluate the conventional knowledge for Si and how it is applied moving forward.

V. ACKNOWLEDGMENTS

The authors thank Thomas M. Jordan of Experimental and Mathematical Physics Consultants (EMPC) for modifying the LAHET code.

VI. REFERENCES

[1] D. Binder, E. C. Smith and A. B. Holman, "Satellite Anomalies from Galactic Cosmic Rays," *IEEE Trans. Nucl. Sci.*, vol. 22, no. 6, pp. 2675-2680, Dec. 1975, doi: 10.1109/TNS.1975.4328188.

[2] Z. Lei, H. Guo, M. Tang, C. Zeng, H. Chen and Z. Zhang, "Heavy ions irradiation effects on AlGaN/GaN high electron mobility transistors," *2016 16th European Conference on Radiation and Its Effects on Components and Systems (RADECS)*, Bremen, 2016, pp. 46-49, doi: 10.1109/RADECS.2016.8093107.

[3] S. Kuboyama et al., "Single-Event Damages Caused by Heavy Ions Observed in AlGaN/GaN HEMTs," *IEEE Trans. Nucl. Sci.*, vol. 58, no. 6, pp. 2734-2738, Dec. 2011, doi: 10.1109/TNS.2011.2171504.

[4] N. A. Vega et al., "Outstanding Reliability of Heavy-Ion-Irradiated AlInN/GaN on Silicon HFETs," *IEEE Trans. Nucl. Sci.*, vol. 66, no. 12, pp. 2417-2421, Dec. 2019, doi: 10.1109/TNS.2019.2954216.

[5] S. E. Armstrong et al., "Heavy Ion Testing of Commercial GaN Transistors in the Radio Frequency Spectrum," *2015 IEEE Radiation Effects Data Workshop (REDW)*, Boston, MA, 2015, pp. 130-135, doi: 10.1109/REDW.2015.7336715.

[6] S. Bazzoli, S. Girard, V. Ferlet-Cavrois, J. Baggio, P. Paillet and O. Duhamel, "SEE sensitivity of a COTS GaN transistor and silicon MOSFETs," *2007 9th European Conference on Radiation and Its Effects on Components and Systems*, Deauville, 2007, pp. 565-569, doi: 10.1109/RADECS.2007.5205553.

[7] M. Zerarka, P. Austin, A. Bensoussan, F. Morancho and A. Durier, "TCAD Simulation of the Single Event Effects in Normally-OFF GaN Transistors After Heavy Ion Radiation," *IEEE Trans. Nucl. Sci.*, vol. 64, no. 8, pp. 2242-2249, Aug. 2017, doi: 10.1109/TNS.2017.2710629.

[8] K. LaBel and J. Pellish, "Domestic Proton Single Event Effects (SEE) Test Facility Status >200 MeV-June 2018," presented at the *2018 NEPP Electronics Technology Workshop*, NASA GSFC, Greenbelt, MD, June 18-21, 2018.

[9] D. M. Hiemstra and E. W. Blackmore, "LET spectra of proton energy levels from 50 to 500 MeV and their effectiveness for single event effects characterization of microelectronics," *IEEE Trans. Nucl. Sci.*, vol. 50, no. 6, pp. 2245–2250, Dec. 2003.

[10] P. O'Neill, G. Badhwar, and W. Culpepper, "Risk assessment for heavy ions of parts tested with protons," *IEEE Trans. Nucl. Sci.*, vol. 44, no. 6, pp. 2311–2314, Dec. 1997.

[11] R. Ladbury, J.-M. Lauenstein, and K. P. Hayes, "Use of proton SEE data as a proxy for bounding heavy-ion SEE susceptibility," *IEEE Trans. Nucl. Sci.*, vol. 62, no. 6, pp. 2505–2510, Dec. 2015.

[12] Z. Wu and S. Chen, "Heavy Ion, Proton, and Neutron Charge Deposition Analyses in Several Semiconductor Materials," *IEEE Trans. Nucl. Sci.*, vol. 65, no. 8, pp. 1791-1799, Aug. 2018.

[13] J. F. Ziegler et al., *The Stopping and Range of Ions in Matter*. Available: http://www.srim.org, December 14, 2020.

[14] D.B. Pelowitz, Ed., "MCNPX Users Manual Version 2.7.0" LA-CP-11-00438 (2011), https://mcnp.lanl.gov/, September 2020.

[15] L. S. Waters et al., "The MCNPX Monte Carlo Radiation Transport Code," *AIP Conference Proceedings*, vol. 896, no. 1, pp. 81-90, 2007, doi: 10.1063/1.2720459

[16] F. Roccaforte et al., "Physics and technology of gallium nitride materials for power electronics," Nuovo Cimento Rivista Serie., vol. 41, no. 12, pp. 625-681, Dec. 2018.

[17] R. Prael and H. Lichtenstein, "User Guide to LCS: The LAHET Code System," Los Alamos Nat. Lab., LA-UR-89–3014, 1989.

[18] S. K. Höeffgen, S. Metzger, and M. Steffens, "Investigating the Effects of Cosmic Rays on Space Electronics," *Frontiers in Physics*, vol. 8, art. no. 318, Sept. 2020, doi: 10.3389/fphy.2020.00318

[19] J. Du, P. Pan, Z. Bai, N. Chen and Q. Yu, "High breakdown voltage AlGaN/GaN HEMTs with nanoscale compound A1 mole fraction barrier layer," *2016 IEEE International Nanoelectronics Conference (INEC)*, Chengdu, 2016, pp. 65-66, doi: 10.1109/INEC.2016.7589283.

[20] S. Bajaj, T. Hung, F. Akyol, D. Nath, and S. Rajan, "Modeling of high composition AlGaN channel high electron mobility transistors with large threshold voltage," *Appl. Phys. Lett.*, vol. 105, no. 26, art. no. 263503, Dec. 2014, doi: 10.1063/1.4905323

[21] G. Baca, A. M. Armstrong,A. A. Allerman, E. A. Douglas, C. A. Sanchez, M. P. King, et al, "An AlN/Al0.85Ga0.15N high electron mobility transistor," *Appl. Phys. Lett.*, vol. 109, no. 3, art. no. 033509, July 2016, doi: 10.1063/1.4959179

[22] R. L. Ladbury and J.-M. Lauenstein, "Evaluating Constraints on Heavy-Ion SEE Susceptibility Imposed by Proton SEE Testing and Other Mixed Environments," *IEEE Trans. Nucl. Sci.*, vol. 64, no. 1, pp. 301-308, Jan. 2017, doi: 10.1109/TNS.2016.2640948.

[23] E. Mizuta et al., "Single-Event Damage Observed in GaN-on-Si HEMTs for Power Control Applications," *IEEE Trans. Nucl. Sci.*, vol. 65, no. 8, pp. 1956-1963, Aug. 2018, doi: 10.1109/TNS.2018.2819990.

[24] Lu Liu et al "Dependence on proton energy of degradation of AlGaN/GaN high electron mobility transistors," *J. Vac. Sci. Technol*., vol. 31, no. 1, art. no. 022201, Jan. 2013, https://doi.org/10.1116/1.4788904

[25] C. Abbate, M. Alderighi, S. Baccaro, G. Busatto, M. Citterio, P. Cova, N. Delmonte et al. "Radiation performance of new semiconductor power devices for the LHC experiment upgrades." In RD13: international conference on Large scale applications and radiation hardness of semiconductor detectors, pp. 1-7. SISSA, 2013.

[26] A. Ionascut-Nedelcescu, C. Carlone, A. Houdayer, H. J. von Bardeleben, J. -. Cantin and S. Raymond, "Radiation hardness of gallium nitride," *IEEE Trans. Nucl. Sci.*, vol. 49, no. 6, pp. 2733-2738, Dec. 2002, doi: 10.1109/TNS.2002.805363.

[27] R. Jiang et al., "Worst-Case Bias for Proton and 10-keV X-Ray Irradiation of AlGaN/GaN HEMTs," *IEEE Trans. Nucl. Sci.*, vol. 64, no. 1, pp. 218-225, Jan. 2017, doi: 10.1109/TNS.2016.2626962.

[28] J. Chen et al., "Effects of Applied Bias and High Field Stress on the Radiation Response of GaN/AlGaN HEMTs," *IEEE Trans. Nucl. Sci.*, vol. 62, no. 6, pp. 2423-2430, Dec. 2015, doi: 10.1109/TNS.2015.2488650.

[29] J. Chen et al., "Proton-Induced Dehydrogenation of Defects in AlGaN/GaN HEMTs," *IEEE Trans. Nucl. Sci.*, vol. 60, no. 6, pp. 4080-4086, Dec. 2013, doi: 10.1109/TNS.2013.2281771.

[30] M. A. Xapsos, C. Stauffer, G. B. Gee, J. L. Barth, E. G. Stassinopoulos and R. E. McGuire, "Model for solar proton risk assessment," *IEEE Trans. Nucl. Sci.*, vol. 51, no. 6, pp. 3394-3398, Dec. 2004, doi: 10.1109/TNS.2004.839159.